

Dehalogenation of 5-Halouracils after Low Energy Electron Attachment: A Density Functional Theory Investigation

Xifeng Li,[†] Léon Sanche,[†] and Michael D. Sevilla*

Group of the Canadian Institutes of Health Research in the Radiation Sciences, Faculty of Medicine, Université de Sherbrooke, Quebec, J1H 5N4, Canada, and Department of Chemistry, Oakland University, Rochester, Michigan 48309

Received: July 19, 2002; In Final Form: September 9, 2002

In this density functional theory investigation of the radiosensitization properties of 5-halogen-substituted uracils, the potential energy surfaces of the halouracils before and after electron attachment are investigated. The electron affinities (EA's) of uracil, halouracils, and uracilyl radical (U-yl[•]) are calculated. The gas-phase adiabatic EA's of the halouracils after zero point energy (ZPE) corrections are in good agreement with those reported recently (Wetmore, S. D.; Boyd, R. J.; Eriksson, L. A. *Chem. Phys. Lett.* **2001**, *343*, 151–158). The U-yl[•] radical has an exceptionally high AEA of 2.34 eV and proton affinity of 9.5 eV in the gas phase, showing its reactive nature and potential to cause DNA damage when incorporated in the genome. The higher EA of the halouracils compared to that of the DNA bases supports the experimental reports on the increased probability of low-energy electrons to localize on halouracils in DNA, leading to dehalogenation reactions and DNA damage. Potential energy surfaces (PES) are calculated for dehalogenation to show the relative energy change in the dissociation of halogen from both the neutral molecule and anion radical. The PESs along the C₅–X bond of all neutral molecules including uracil show the typical surface expected for a strong covalent bond rupture. Each of the halouracil anion radicals is found to have two thermally accessible electronic states of differing symmetries, i.e., $\pi^*(A'')$ and $\sigma^*(A')$, that have quite differing properties. Both the pure π^* state and the σ^* state feature planar geometries. The pure π^* state has a PES similar to that of the neutral molecule with a strong C–X bond, while the σ^* state shows far weaker C–X bonding. Moreover, there is a mixed state PES that undergoes a transition from a slightly nonplanar π^* state to that of a σ^* state as the C–X bond distance increases to the crossing point of the two PES. From the full PES that allows for state crossing, the lowest energy barriers for formation of the extended σ^* states are estimated to be 20.80, 3.99, and 1.88 kcal/mol for F-, Cl-, and Br-substituted uracil anion radicals, respectively. The overall energetics suggest that the π^* to σ^* conversions are exothermic for ClU and BrU anions, with ΔH calculated to be –0.98 and –2.98 kcal/mol, ΔG , –2.32 and –3.80 kcal/mol at 298 K and 1 atm, respectively. Remarkably, for the F–U anion the lowest energy path is not the loss of fluoride ion but the detachment of HF. The sensitivity of the halouracils to low-energy electrons is found to be on the order of BrU \approx ClU \gg FU, in agreement with experimental observations.

Introduction

The radiosensitization properties of 5-halogen-substituted uracils, such as 5-BrU, have been well recognized and employed in radiation therapy.^{1–5} As analogues of thymine, these 5-halogenated uracils can be easily incorporated into DNA in place of thymine.⁶ Ionizing radiation⁷ and more recently low-energy electrons⁸ have been found to cause damage to normal DNA. With incorporation of halogenated uracils in DNA the damage is enhanced and results in significant increase of cell death. The mechanism of radiosensitization is considered to be a result of attachment to the halouracil of secondary electrons which are produced in large amounts by ionizing radiation. This attachment results in dehalogenation and formation of the very reactive uracil-5-yl radical,⁹ which subsequently can cause DNA strand breaks. However, mechanistic details of the process are not fully understood.

A variety of experiments have shown that halogen anions and uracilyl radicals are the products of the interaction of high-energy (MeV) electrons,¹⁰ γ -ray,¹¹ subionization (0–10 eV) electron beams,^{9,12,13} or X-ray¹³ with halouracils and halogenated DNA. Several dissociation pathways have been proposed^{12a} to explain the fragmentation of halouracils after reaction with the electron. The dehalogenation of halouracils had been shown to proceed via the capture of an electron to form a transient anion which dissociates into a halide anion and a uracilyl radical. This process is called *dissociative electron attachment* (DEA).^{14,15} In diluted aqueous solutions, the captured species is the solvated electron.¹⁰ In gas⁹ and solid¹³ phase experiments, it has recently been shown that nonthermalized low-energy secondary electrons (LEE), which are produced in abundance by high-energy radiation, are captured by the halouracils to form the transient anion. Metastable anion radicals of BrU or ClU were found to exist at low temperatures from ESR experiment; they undergo dehalogenation on temperature rise or light exposure.^{11a,16,17}

The dehalogenation leaves behind the very reactive radical U-yl[•] or an anion (U-yl)[–] and a reactive halogen radical.

* Corresponding author: Oakland University. E-mail: sevilla@oakland.edu. Telephone: (248)370-2328. Fax: (248)370-2321.

[†] Université de Sherbrooke.

TABLE 1: Electron Affinity of 5-Substituted Uracils (eV) Calculated at B3LYP/6-31+G(d)

correction	gas-phase AEA			solvated AEA		VEA		VDE none
	none	ZPE	ref 18	none	ref 18	none	ref 18	
phase	gas	gas	gas	IPCM	PCM	gas	gas	gas
uracil	0.066	0.184	0.18	2.02	2.30	0.35	0.26	0.76
5-FU	0.37	0.48	0.45	2.21	2.42	0.15	0.03	1.14
5-CIU	0.49	0.60	0.58	2.26	2.53	0.06	0.14	1.20
5-BrU	0.51	0.63	0.64	2.44	2.60	0.11	0.17	1.21
U-yl	2.30	2.34		4.47		1.89		2.74

Recently, Abdoul-Carime et al.⁹ estimated the branching ratios, $U\text{-yl}^{\bullet}/X^{\bullet}$ ($X = \text{Br}, \text{Cl}, \text{or I}$) for the gas-phase production of these reactive radicals from 5-CIU, 5-BrU, and 5-IU to be 1.3, 40, and 490, respectively. They also reported that $U\text{-yl}^{\bullet}$ has a high electron affinity (equivalent to vertical detachment energy, VDE) of 3.2–3.5 eV. Furthermore they found that 0–3-eV electrons resulted in more $U\text{-yl}^{\bullet}$ from 5-BrU than from 5-CIU or 5-IU, while most free halogen radical arises from 5-CIU. No F^{\bullet} dissociated from 5-FU by electron attachment below ~ 2 eV.¹³ According to the mechanism postulated by Boudaiffa et al.⁸ for LEE damage to DNA, DEA can lead to both single- and double-strand breaks. With the present dehalogenation process, a single-strand break can occur from the reaction of a $U\text{-yl}^{\bullet}$ radical or a halogen atom. To break two strand in a single DEA event, however, one of the fragments has to react with the opposite strand.

In contrast to the large number of experimental efforts, theoretical reports are rare despite the strong need to further understanding the radiosensitization properties of these halouracils. The first detailed theoretical report¹⁸ appeared only recently by Wetmore et al. They reported the calculated values of electron affinity (EA), the ionization potential (IP) in gas phase and solution, and the barriers for dissociation of the $5XU$ anions into X^{\bullet} plus the $U\text{-yl}^{\bullet}$ radical decrease in order of $5\text{-FU}^{-} > 5\text{-CIU}^{-} > 5\text{-BrU}^{-}$.

In this work, we employ the density functional theory (DFT) method to explore the energetics of dehalogenation after attachment of an electron to halouracils (5-FU, 5-CIU, and 5-BrU) in the gas phase and in water solution, with the aim of providing more details on the potential energy surfaces (PES) important to the fragmentation of these molecules after electron attachment, including uracil for comparison, and the properties of the reactive $U\text{-yl}^{\bullet}$ radical.

Terms: The adiabatic electron affinity (AEA) is defined as the energy difference between the neutral species and the anion each in equilibrium geometry. The vertical electron affinity (VEA) is the energy difference between neutral and anion both with the internuclear position of the equilibrium neutral geometry. The vertical detachment energy (VDE) is the energy required to remove an electron from the optimized anion, without causing geometry change. It is thus the energy difference between the optimized anion and the neutral in the anion geometry.

Calculation Methods

Unless stated otherwise, all calculations were performed by using the DFT B3LYP functionals with the 6-31+G(d) basis set provided in the Gaussian 98 program package.¹⁹ The accuracy of this level of theory has been well-demonstrated elsewhere.²⁰ All geometries of the 5-X-uracils, where $X = (\text{H}, \text{F}, \text{Cl}, \text{or Br})$ and $U\text{-yl}^{\bullet}$ radical, were optimized in gas phase. Frequency calculations (without scaling) were performed to obtain zero-point corrections to energy (ZPE). The AEA is calculated by the difference of the energy of the optimized neutral minus that of the optimized anion.

The energies of the 5-X-uracils in solvated environment were calculated by using the isodensity PCM model (SCRF=IPCM)²¹ for water as solvent. Geometries optimized in the gas phase were used. The electron affinities in solvated environment were calculated by using the resulted energies; no ZPE corrections were made.

Adiabatic potential energy surfaces (PES) along the C–X bond stretch were calculated by using optimization keyword `opt = ModRedundant` and included the S action code in the additional input. Unlike the SCAN method which performs a rigid PES scan without geometry optimization, the S action code causes geometry optimization for each point along the specified range of C–X distances, from ~ 1 Å up to 3.0 Å. The optimized geometries found along the C–X coordinates were further verified by frozen C–X distance optimizations, which also served to obtain information about the charge/spin distributions and molecular orbital symmetry. PES scans for neutral halouracils used the `guess = mix` option to allow for unrestricted calculations needed for appropriate dissociation limits.

Results & Discussion

Electron Affinity of 5-Halouracils. Table 1 lists the electron affinities we calculated at the b3lyp/6-31+g(d) level, for uracil, the 5-halo uracils, and the $(U\text{-yl})^{\bullet}$ radical. Values obtained by Wetmore et al.¹⁸ are listed together for comparison. As can be seen, the results we obtained are in good agreement with those of Wetmore's¹⁸ on the values of gas-phase adiabatic EA as well as vertical EA, despite that they used a larger basis set: B3LYP/6-311+G(2df,p). The discrepancy on AEA in solution arises mostly from the use of different models besides the different basis set size. The PCM model²² was used by Wetmore et al., while we use the improved IPCM model.²¹ The general agreement is that the EA values are all in the following relative order: $U\text{-yl}^{\bullet} \gg \text{BrU} > \text{CIU} > \text{FU} \gg \text{U}$. Even in a solvated environment, this relative order is maintained. Since the adiabatic EA of uracil is among the highest of all the natural DNA/RNA bases,^{20a} these results confirm the long-held assumption that the halouracils are more powerful electron scavengers than natural bases when they are present in DNA. While halouracils in DNA are likely to possess the largest reaction rates toward direct electron capture of radiation-produced excess electrons, the most probable route of electron attachment to halouracils is by electron transfer²³ from the far more abundant but less electron affinic DNA bases. In effect, the DNA captures and funnels electrons to the halouracils, resulting in DNA damage from a normally harmless agent, i.e., a radiosensitization effect.

The $U\text{-yl}^{\bullet}$ radical has an exceptionally high adiabatic EA, which is calculated to be 2.34 eV in the gas phase with ZPE correction and 4.47 eV in solvated environment. From experiment, Abdoul-Carime et al.⁹ found its gas-phase VDE falls in the range of 3.2–3.5 eV. Our VDE value is calculated to be 2.74 eV without ZPE correction. The ZPE correction may bring it to around 3 eV, but such corrections are theoretically problematic for nonrelaxed systems. The important point here

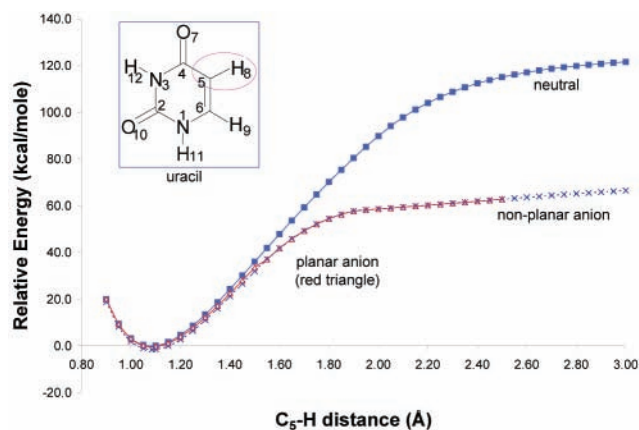


Figure 1. Potential energy surfaces (PES) of uracil and its anion radical along the C₅-H bond. The energy of the optimized uracil neutral molecule is set as reference. The C₅-H bond is circled in the structure.

TABLE 2: Equilibrium C-X Distance of 5-X-Uracils in Gas Phase (Å)

X =	anion radical				
	neutral	π^* (planar)	π^* (nonplanar)	transition	σ^* minimum
H	1.082	1.085	1.085		
F	1.344	1.382	1.383	2.093	2.131
Cl	1.733	1.766	1.771	2.041	2.607
Br	1.878	1.903	1.918	2.147	2.614

is that both theory and experiment give a very high electron affinity for U-yl[•]. U-yl[•] is very reactive and can react easily with its surroundings (e.g., by H-abstraction leading to a DNA single-strand break). Of course, with its large EA it may also be involved in one-electron oxidations to form the U-yl⁻.

It should be pointed out that, as discussed below, each of the 5-X uracil anion radicals has more than one energy minimum, corresponding to differing symmetry states. Typically, there is a pure π^* state that features a planar geometry, a very slightly lower energy π^* -type (but mixed) state with a nonplanar local minimum, and finally a σ^* dissociative state. In their optimized π^* planar geometries, two negative imaginary frequencies are found for each of the anion radicals, indicating that these planar anion radicals are at a saddle point. These structures relax into a slightly nonplanar geometry which is still π^* in nature. Both our values and those from Wetmore et al.¹⁸ in Table 1 are those for the anion radicals in nonplanar optimized geometries.

Potential Energy Surfaces (PES) of Neutral Molecules. All the neutral 5-X uracil molecules, are found to be in planar geometries at equilibrium and at any point on the potential energy surface (PES). The equilibrium C-X distances in gas phase are listed in Table 2. The PES of the neutral molecule along the C-X bonds are similar and follow the typical Morse potential shape, in that each of the surfaces has only one minimum and the relative energy increases monotonically as C-X bond is stretched. Figure 1 shows the PES along the C₅-H bond for uracil and its anion radical. For convenience, a numbered structure is included and the C₅-H bond is circled. Figure 2 shows the same information for 5-BrU, Figure 3 for 5-ClU, and Figure 4 for 5-FU, respectively.

Potential Energy Surface (PES) of Anion Radicals and the Dissociation of Halogens. The potential energy surfaces for the halouracil anion radicals are shown in Figures 1-4 and discussed individually below.

Uracil (Figure 1). The PES of the neutral uracil along C₅-H bond stretch shows an energy surface typical of a strong covalent

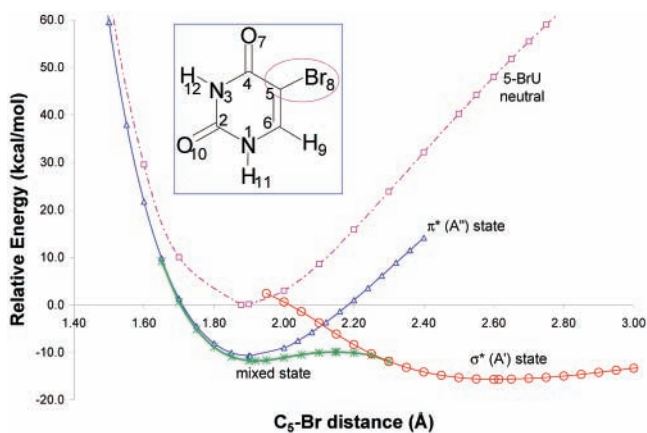


Figure 2. Potential energy surfaces (PES) of 5-Br-uracil and its anion radical along the C₅-Br bond. The energy of the optimized neutral molecule is set as reference. The C₅-Br bond is circled in the structure.

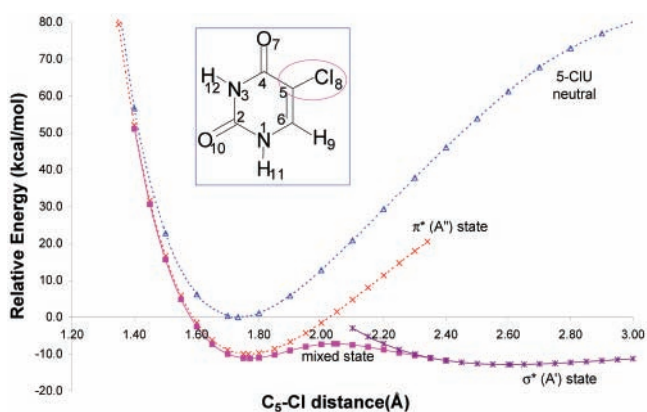


Figure 3. Potential energy surfaces (PES) of 5-Cl-uracil and its anion radical along the C₅-Cl bond. The energy of the optimized neutral molecule is set as reference. The C₅-Cl bond is circled in the structure.

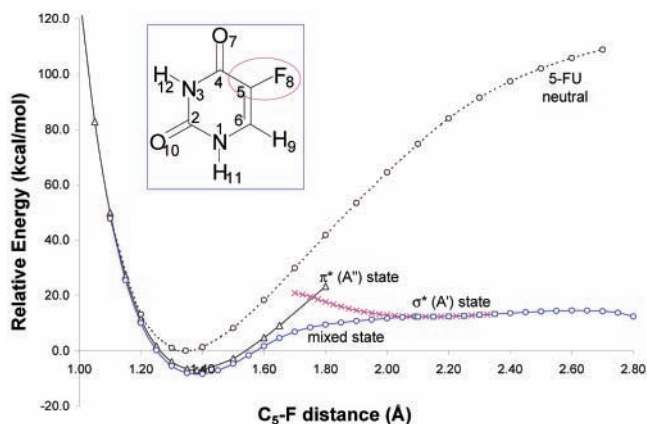


Figure 4. Potential energy surfaces (PES) of 5-fluorouracil and its anion radical along the C₅-F bond. The energy of the optimized neutral molecule is set as reference. The C₅-F bond is circled in the structure.

bond, for which we estimate a bond enthalpy of ~ 117.3 kcal/mol (see below). The energy surface for the dissociation of the anion radical to U-(5)yl⁻ radical and hydrogen atom is weaker and approaches a maximum of ca. ~ 70 kcal/mol. This remains a substantial energy barrier and autodetachment of H(C₅) in the uracil anion radical would be a highly energetic and unlikely process. Two anion PES were calculated for the C-H distances smaller than 1.5 Å, corresponding to the anion in planar or lower energy nonplanar geometry, respectively. The two surfaces merge into one as the nonplanar geometry becomes planar beyond 1.5 Å. The energy difference between the two calculated

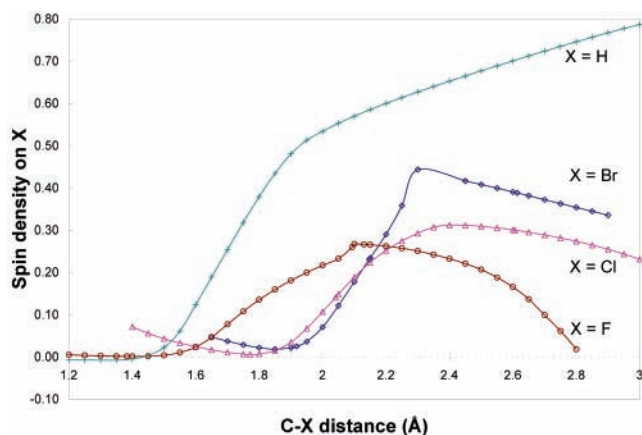


Figure 5. Spin density on X (X = H, Br, Cl, or F) along the anion radical PESs of uracil and along the mixed state surfaces for halouracils. A complete set of data is available in the supporting information.

surfaces is very small; for example, the nonplanar geometry minimum lies only 1.13 kcal/mol lower than the planar minimum. Remarkably, the energy of the optimized neutral lies only 0.38 kcal/mol above that of the optimized planar anion with nearly the same bond distance. The fact that most stable state of the uracil anion is calculated to be a nonplanar geometry is in agreement with the recent study²⁴ using a higher level of theory.

Figure 5 shows that the spin density on H increases as the C–H distance increases beyond 1.5 Å. At 3.0 Å, the spin density on H reaches 0.787, with very little negative charge on H. This indicates that it is departing as a hydrogen atom, rather than a hydride ion. The turning point between 1.90–1.95 Å is accompanied by a drastic shift of spin from C₆ to C₅ in keeping with the change from a π^* state to the dissociative σ^* state. A complete listing of charge/spin is available as Supporting Information.

The proton affinity (PA)²⁵ is defined as the energy released on proton addition to a molecule. We calculated this value to be 9.5 eV or 220 kcal/mol for the U-yl[•] radical, $PA = E(U-yl^+) - E(U^+)$. The bond energy of U–H to form the U-yl[•] radical and a free hydrogen atom amounts to 5.1 eV (117.3 kcal/mol), a value which suggests a strong tendency of the radical to abstract H from its neighbor.

5-Bromouracil (Figure 2): The PES of BrU anion radical along the C–Br bond is complicated by the fact that the radical has two intersecting PESs of differing symmetry: a $\pi^*(A'')$ state and a $\sigma^*(A')$ state. The π^* state consists of a singly occupied molecular orbital (SOMO) with A'' symmetry, while that for the σ^* state has A' symmetry. The π^* state does relax to a slightly nonplanar form but maintains the π^* nature although it of course loses A'' symmetry.

The PES of the $\pi^*(A'')$ state is similar to that of neutral BrU, which has a Morse potential shape expected for a strong covalent bond but lies slightly below the neutral species in energy owing to its' positive electron affinity (Figure 2). The C–Br distance at equilibrium is 1.903 Å (Table 2). For the planar $\pi^*(A'')$ state, calculations could not be performed beyond a C–Br distance of ~2.4 Å at which the calculations fail to maintain the π^* symmetry. The “pure” σ^* state also features a planar geometry, with an equilibrium C–Br distance of 2.614 Å (Table 2). Besides these two pure states, there is also a lower-energy PES that initially starts with a nonplanar geometry of π^* nature. At the crossing point of the two pure surfaces, this π^* state shifts to the σ^* state PES. At longer distance the geometry resumes planarity and the PES merges into the pure σ^* state PES (Table

TABLE 3: Energetics of Dehalogenation Reactions from Halouracil Anion Radicals at 298 K, 1 Atm, Gas Phase (kcal/mol)

anion	activation energy ^a	ΔH_{\min}^b	ΔH_{∞}^b	ΔG_{\min}^b	ΔG_{∞}^b	ΔE_{∞}^c
5-FU	20.80 (22.23) ^a	20.82	37.46	19.01	27.44	49.6 ^c (51.9) ^d
5-ClU	3.99 (4.57)	0.98	18.28	2.32	10.51	18.0 (20.2) ^d
5-BrU	1.88 (0.26)	2.98	21.20	3.80	13.29	21.0 (12.6) ^d

^a ZPE corrections not included for E_a , values in parentheses from ref 18 with ZPE correction included. ^b Values for minima are those for the extended σ^* state, while those at infinity are for full separation of the halouracil anion to U-yl[•] and Br⁻ or Cl⁻ for ClU⁻ or to U-5,6-yl[•] and HF for FU⁻. ^c Energy change for $XU^- \rightarrow U-yl^+ + X^-$ at infinite separation. For 5-FU case the separation is also computed for F⁻ formation not HF. ^d Values in parentheses from ref 18 for $XU^- \rightarrow U-yl^+ + X^-$ at infinite separation.

2, Figure 2). The nonplanar π^* anion has a C–Br distance of 1.918 Å at equilibrium, slightly longer than that in planar geometry (1.903 Å). The transition point from one symmetry type to another is found at 2.147 Å. The distances of nonplanar minimum, transition states, and the σ^* state minimum are in excellent agreement with those reports by Wetmore et al.¹⁸ They, however, did not report the planar $\pi^*(A'')$ potential energy surface or that for the σ^* state. The σ^* minima corresponds to their “product complexes”.

At equilibrium, the neutral 5-Br-uracil is in the planar geometry. After attachment of an electron, the anion initially is in the planar geometry, which corresponds to the pure π^* state. The anion in this π^* state is not stable as it is found to have two negative frequencies, and the adiabatic EA calculated based on this anion's energy is 0.46 eV without ZPE correction and 0.62 eV with correction. The dissociation of Br in the π^* state is energetically unfavorable as can be seen from the pure π^* state PES (Figure 2). The relaxation of the anion results in the loss of planarity on forming the slightly lower energy π^* -type state. The adiabatic EA's calculated based on this anion's energy are similar to the planar form (i.e., 0.51 eV without correction and 0.63 eV with correction); see Table 1.

Spin density on Br as a function of C–Br distance is shown in Figure 5. In the π^* state there is little spin density on Br and it decreases as C–Br distance increases till the spin density is virtually zero where the state breaks down. On the mixed-state PES, the charge/spin density distributions suggest that the unpaired spin falls mostly on C₆ initially, as expected for the π^* state. As the C–Br distance increases, the unpaired spin shifts and is shared between C₅ and Br as expected for the σ^* state. At ~2.30 Å, the spin density on Br reaches a maximum of 0.444. On further increase of the distance the spin falls mostly on C₅ as expected for a bond rupture. With the shift in spin to C₅, we find that the negative charge shifts to Br as the C–Br distance increases. At C–Br = 5 Å, the charge on Br is -0.74 and the spin is 0.25. These tendencies of charge/spin distribution suggest that bond cleavage of the BrU anion is more likely to result in a Br⁻ ion and a U-yl[•] radical, rather than a Br[•] radical and U-yl⁻. This is in keeping with the relative electron affinities of the two species.

The overall PES predicts that the conversion to the weakly associated σ^* state has only a small activation barrier of 1.88 kcal/mol (no ZPE correction, Table 3) to reach the transition state at C–Br = 2.147 Å. This barrier is only slightly larger than the 0.26 kcal/mol, which includes the ZPE correction reported by Wetmore et al. The overall reaction is calculated to be exothermic with $\Delta H = -2.98$ kcal/mol and favorable with $\Delta G = -3.80$ kcal/mol at 298 K, 1 atm, from the difference of the σ^* state and nonplanar minimum (π^* -type state). However,

separation of U-yl* and Br⁻ at infinity in the gas phase is energetically unfavorable, which leads to 20.96 kcal/mol increase of the total energy.

5-Chlorouracil (Figure 3). The PES of the CIU anion is similar to that of BrU anion: a pure π^* (A'') state PES and an intersecting pure σ^* (A') state PES, both featuring planar geometry. The pure π^* PES has minimum at C–Cl = 1.766 Å, while the σ^* PES has its minimum at 2.607 Å (Table 2). The mixed-state PES initially starts with a nonplanar geometry of π^* nature and shifts to the σ^* state PES at the crossing point of the two pure surfaces. At equilibrium, the nonplanar anion is more stable and has a slightly longer C–Cl distance of 1.771 Å than the pure π^* state minimum. The transition point is found at C–Cl = 2.041 Å, beyond that it gradually merges into the pure σ^* state PES (Table 2, Figure 2). Again the distances are in excellent agreement with those reported by Wetmore et al.,¹⁸ except that they did not report the pure π^* state (planar saddle point). The change in the spin/charge distribution (Figure 5) on Cl with the C–Cl distance is similar to that in the BrU anion. At short distances, the spin falls mostly on C₆ with little spin density on Cl; as distance increases, the spin is increasingly shared between C₅ and Cl and finally it lies mainly on C₅. The spin density on Cl reaches a maximum of 0.312 at ~2.40 Å, and at larger distances it decreases, while at the same time the negative charge on Cl increases. At 3.0 Å, the charge on Cl is -0.73 and the spin density is 0.23. These tendencies are in keeping with a cleavage of C–Cl bond in the CIU anion radical that ends with the formation of a U-yl* radical and Cl⁻ ion, as found for the BrU anion radical. The energetics of the initial step in the dehalogenation reaction from the CIU anion, based on the mixed state PES, suggests an activation energy barrier of 3.99 kcal/mol (Table 3), which is close to the ZPE corrected value of 4.57 kcal/mol reported by Wetmore et al.¹⁸ These values are over twice that found here for BrU anion. The overall dehalogenation process for CIU anion is exothermic with $\Delta H = -0.98$ and $\Delta G = -2.32$ kcal/mol at 298 K, 1 atm (Table 3), though slightly less exothermic than for the BrU anion. However, as found for the Br–U anion radical, complete separation of U-yl* and Cl⁻ is also energetically unfavorable and needs 17.98 kcal/mol of energy in the gas phase. The greater exothermicity calculated for BrU anion is in accord with experimental observations⁹ from low-energy electron impact studies of gas-phase halouracils.

5-Fluorouracil (Figure 4). The PESs of the FU anion are similar to those of BrU and CIU anions in that we find a pure π^* surface, a mixed state surface starting with a slightly nonplanar π^* state and ending with the σ^* state, and a pure σ^* surface. The equilibrium C–F distances of the three states are 1.382, 1.383, and 2.131 Å, respectively (Table 2). The transition point along the PES is found at 2.093 Å, which is very close to the σ^* -minimum and even longer than that of the CIU anion. In fact, the transition point is nearly on the σ^* -state PES. These distances are also in excellent agreement with those reported by Wetmore et al.,¹⁸ of course except the pure π^* state (saddle point).

Figure 6 shows the geometry change of the FU anion along the mixed-state PES. These geometry changes with C–F bond stretching indicate that beyond the σ^* state minimum (2.131 Å), the incipient fluoride ion approaches the neighboring H on C₆ and the C–H bond is weakened with the increase of C–F distance. At C–F = 2.80 Å, the distance between F and H is only 1.07 Å, about the normal bond distance in the HF molecule. The X–H bond formation is not found in the cases of BrU and CIU anions. The nonplanar halogen seen up to the σ^* state

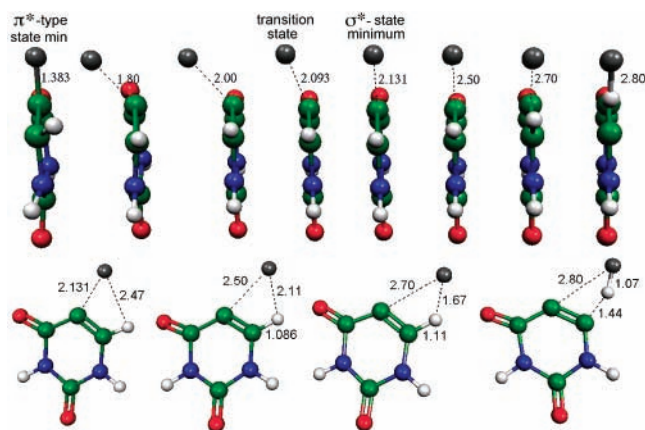


Figure 6. Edge views of the geometry changes for the 5-fluorouracil anion radical along the mixed-state potential energy surface. Face views better depict the gradual dissociation of hydrogen fluoride with C–F bond extension from 2.13 Å (the σ^* state minimum) to 2.80 Å at which H–F clearly forms.

minimum is common to all the halouracil PES. In the separated state, the relative energy of the HF molecule plus the U-5,6-yl anion radical to the 5-FU anion radical is 37.5 kcal/mol (Table 3), which is substantially lower than that of 49.55 kcal/mol (our value) or 51.89 kcal/mol (217.1 kJ/mol) found by Wetmore et al.¹⁸ for formation of U-yl* and F⁻, which is the alternative dehalogenation pathway. It is obvious that, in the gas phase, dehalogenation from the FU anion is not likely to occur. If it does occur, our calculations predict it will result in a HF molecule and U-5,6-yl anion radical. This is in good agreement with experimental observations that dehalogenation from 5-FU does not occur by attachment of electrons with energies below ~2 eV.¹³ At C–F distances below 1.5 Å, the spin density on fluorine is negligible in either the pure π^* state PES or the nonplanar π^* -type state PES (Figure 5). Most of the spin density is found to be in the 2p_z atomic orbital on C₆. As distance increases, the spin shifts to be “shared” between C₅ and F, but mostly it is on C₅. The spin density on fluorine reaches a maximum of 0.267 at 2.1 Å, at a C–F distance between the transition state and the σ^* minimum. After this distance, the spin on fluorine declines rapidly. At the same time, the negative charge on F increases steadily until 2.7 Å, where it reaches -0.76. Remarkably, after 2.7 Å, the formation of HF molecule becomes obvious as the distance between H and F decreases and the total spin density and excess charge on these atoms becomes negligible.

Summary

The gas-phase adiabatic electron affinities with ZPE corrections in electronvolts are U-yl* (2.34) \gg 5-BrU (0.63) > 5-CIU (0.60) > 5-FU (0.48) \gg uracil (0.184). The same relative order is also found for estimates for adiabatic EA's in solution (IPCM model), vertical EA, and vertical detachment energies. The halouracils have higher electron affinities than all natural bases. These results for the halouracils are in good agreement with the earlier work of Wetmore et al.¹⁸

In the gas phase, the U-yl* radical is found to have an exceptionally high adiabatic EA (2.34 eV, ZPE corrected), vertical detachment energy (VDE, 2.74 eV, without ZPE correction), proton affinity (9.5 eV), and bond dissociation energy (5.1 eV) for U–H to form the U-5-yl• radical and H•. These values clearly demonstrate the reactive nature of the radical.

All the halouracil anions in the gas phase are found to have multiple *thermally accessible* electronic states: a pure π^* state

(SOMO in A'' symmetry), a π^* -type mixed state and a pure σ^* state (SOMO in A' symmetry). All pure π^* and σ^* PES feature a planar geometry. The minimum energy mixed-state PES starts with a π^* -type state with a nonplanar geometry which remains at the transition state but on C–X bond extension converts to a PES with a planar σ^* state. The planar π^* states for the halouracil anion radicals are very slightly higher in energy than the nonplanar π^* -type mixed states; however, experimental evidence from single crystals suggests planar states are likely to be favored within a DNA base stack.²⁶

Formation of the weakly interacting σ^* state of the anion radicals of BrU and CIU requires only small activation energies, which are 1.88 and 3.99 kcal/mol, respectively. Further the reactions are exothermic with $\Delta H = -2.99$ and -0.98 and $\Delta G = -3.80$ and -2.32 kcal/mol, for BrU⁻ and CIU⁻, respectively. However, extension of the U-yl^{*} to X⁻ distance to infinity is found to be energetically unfavorable in every case in the gas phase. In contrast to the BrU and CIU anions, formation of the weakly interacting σ^* state of the FU anion is unfavorable energetically by 20.8 kcal/mol. Moreover, complete separation of U-yl^{*} and F⁻ to infinity is energetically very unfavorable in the gas phase, which needs at least 49.55 kcal/mol (2.14 eV) of energy. This is in good agreement with the earlier calculations¹⁸ and experimental observations that dehalogenation from 5-FU does not occur by attachment of electrons with energies below ~ 2 eV.¹³ The sensitivity of the halouracils to dehalogenation by low-energy electrons is on the order of BrU \approx CIU \gg FU.¹³ In aqueous solution solvation energies were shown by Wetmore et al. to provide sufficient driving force for dissociation so that dehalogenation of every halouracil anion radicals was exergonic.¹⁸

Dehalogenation of BrU and CIU anion radicals most likely leads to formation of the U-yl^{*} radical and halogen anion. For the FU anion radical, bond fragmentation leads to a HF molecule and a U-5,6-yl anion radical, which is less endothermic than the alternative pathway of forming a U-yl^{*} radical and a F⁻ ion.¹⁸ The likely reason that this pathway is available only for the case of FU is the large proton affinity of the F⁻. It is far larger than that of Cl⁻ or Br⁻ (16.15 eV (F⁻) vs 14.45 eV (Cl⁻) and 14.06 eV (Br⁻); NIST WebBook) or apparently the carbon at C-6. Thus the F⁻ leaves with the C-6 proton, whereas the Br⁻ and Cl⁻ anions do not.

We find detachment of hydrogen from C₅ of uracil anion radical leads to formation of U-yl⁻ and a H atom. The hydrogen atom is a poor competitor for the electron with the highly electron affinic U-yl^{*} radical.

Acknowledgment. We gratefully acknowledge many helpful discussions with Maria Szczesniak. This research was supported by the Canadian Institutes of Health Research, the National Cancer Institute of Canada and by the NIH NCI Grant RO1CA45424, in joint efforts between Département de Médecine Nucléaire et Radiobiologie, Université de Sherbrooke, and Department of Chemistry, Oakland University.

Supporting Information Available: Optimized geometries of halouracils/uracil/U-yl^{*} radical and charge/spin density distribution in halouracil anion radicals vs C–X distances. This material is available free of charge via the Internet at <http://pubs.acs.org>.

References and Notes

(1) Zamenhof, S.; DeGiovanni, R.; Greer, S. *Nature* **1959**, *181*, 827

(2) Coleman C. N.; Glover, D. J.; Turrisi, A. T.; Radiation and chemotherapy sensitizers and protectors. In *Cancer Chemotherapy: Principles and Practice*; Chabner, B. A., Collins, J. M., Eds.; Lippincott, J. B.: Philadelphia, 1990; pp 424–447.

(3) Lawrence, T. S.; Davis, M. A.; Maybaum, J.; Stetson, P. L.; Ensminger, W. D. *Radiat. Res.* **1990**, *123*, 192

(4) Kinsella, T. J.; Mitchell, J. B.; Russo, A.; Morstyn, G.; Glatstein, E. *Int. J. Radiat. Oncol.* **1984**, *10*, 1399.

(5) Buchholz, D. J.; Lepek, K. J.; Rich, T. A.; Murray, D. *Int. J. Radiat. Oncol.* **1995**, *32*, 1053.

(6) Szybalsky, W. *Cancer Chemother. Rep.* **1974**, *58*, 539–557.

(7) (a) Becker, D.; Sevilla, M. D. *Adv. Radiat. Biol.* **1993**, *17*, 121–18. (b) Wang, W.; Sevilla, M. D. *Radiat. Res.* **1994**, *138*, 9–17. (c) Sonntag, C. Von. *The Chemical Basis for Radiation Biology*; Taylor and Francis: London, 1987.

(8) Boudaiffa, B.; Cloutier, P.; Hunting, D.; Huels, M. A.; Sanche, L. *Science*, **2000**, *287*, 1658.

(9) Abdoul-Carime, H.; Huels, M. A.; Illenberger, E.; Sanche, L. *J. Am. Chem. Soc.* **2001**, *123*, 5354.

(10) (a) Zimbrick, J. D.; Ward, J. F.; Myers, Jr., L. S. *Int. J. Radiat. Biol.* **1969**, *16*, 505. (b) Zimbrick, J. D.; Ward, J. F.; Myers, L. S., Jr. *Int. J. Radiat. Biol.* **1969**, *16*, 525.

(11) (a) Sevilla, M. D.; Failor, R.; Zorman, G. *J. Phys. Chem.* **1974**, *78*, 696. (b) Razzkazovskii, Y.; Swarts, S. G.; Falcone, J. M.; Taylor, C.; Sevilla, M. D. *J. Phys. Chem. B* **1997**, *101*, 1460. (c) Simpson L. D.; Zimbrick, J. D. *Int. J. Radiat. Biol.* **1975**, *28*, 461.

(12) (a) Dugal, P.-C.; Abdoul-Carime, H.; Sanche, L. *J. Phys. Chem. B* **2000**, *104*, 5610. (b) Abdoul-Carime, H.; Huels, M. A.; Bruning, F.; Illenberger, E.; Sanche, L. *J. Chem. Phys.* **2000**, *113*, 2517. (c) Abdoul-Carime, H.; Dugal, P.-C.; Sanche, L. *Radiat. Res.* **2000**, *153*, 23.

(13) Klyachko, D. V.; Huels, M. A.; Sanche, L. *Radiat. Res.* **1999**, *151*, 177–187.

(14) Sanche, L. *Scanning Microsc.* **1995**, *9*, 619.

(15) Christophourou, L. G. In *Electron–Molecule Interactions and their Applications*; Christophourou, L. G., Ed.; Academic Press: New York, 1984; Vol. 1.

(16) Riederer, H.; Huettermann, J.; Symons, M. C. R. *J. Chem. Soc. Chem. Commun.* **1978**, 313.

(17) Sevilla, M. D.; Swarts, S.; Riederer H.; Huettermann, J. *J. Phys. Chem.* **1984**, *88*, 1601.

(18) Wetmore, S. D.; Boyd, R. J.; Eriksson, L. A. *Chem. Phys. Lett.* **2001**, *343*, 151–158.

(19) Frisch, M. J.; Trucks, G. W.; Schlegel, H. B.; Scuseria, G. E.; Robb, M. A.; Cheeseman, J. R.; Zakrzewski, V. G.; Montgomery, J. A., Jr.; Stratmann, R. E.; Burant, J. C.; Dapprich, S.; Millam, J. M.; Daniels, A. D.; Kudin, K. N.; Strain, M. C.; Farkas, O.; Tomasi, J.; Barone, V.; Cossi, M.; Cammi, R.; Mennucci, B.; Pomelli, C.; Adamo, C.; Clifford, S.; Ochterski, J.; Petersson, G. A.; Ayala, P. Y.; Cui, Q.; Morokuma, K.; Malick, D. K.; Rabuck, A. D.; Raghavachari, K.; Foresman, J. B.; Cioslowski, J.; Ortiz, J. V.; Stefanov, B. B.; Liu, G.; Liashenko, A.; Piskorz, P.; Komaromi, I.; Gomperts, R.; Martin, R. L.; Fox, D. J.; Keith, T.; Al-Laham, M. A.; Peng, C. Y.; Nanayakkara, A.; Gonzalez, C.; Challacombe, M.; Gill, P. M. W.; Johnson, B. G.; Chen, W.; Wong, M. W.; Andres, J. L.; Head-Gordon, M.; Replogle, E. S.; Pople, J. A. *Gaussian 98*, revision A.7; Gaussian, Inc.: Pittsburgh, PA, 1998.

(20) (a) Li, X.; Cai, Z.; Sevilla M. D. *J. Phys. Chem. A* **2002**, *106*, 1596. (b) Rienstra-Kiracofe, J. C.; Tschumper, G. S.; Schaefer III, H. F. *Chem. Rev.* **2002**, *102*, 231.

(21) Foresman, J. B.; Keith, T. A.; Wiberg, K. B.; Snoonian, J.; Frisch, M. J.; *J. Phys. Chem.* **1996**, *100*, 16098.

(22) (a) Miertus, S.; Scrocco, E.; Tomasi, J. *Chem. Phys.* **1981**, *55*, 117. (b) Miertus, S.; Tomasi, *Chem. Phys.* **1982**, *65*, 239. (c) Cossi, M.; Barone, V.; Cammi, R.; Tomasi, J. *Chem. Phys. Lett.* **1996**, *255*, 327.

(23) (a) Cai, Z.; Li, X.; Sevilla, M. D. *J. Phys. Chem. B* **2002**, *106*, 2755. (b) Cai, Z.; Gu, Z.; Sevilla, M. D. *J. Phys. Chem. B* **2001**, *105*, 6031. (c) Cai, Z.; Sevilla, M. D. *J. Phys. Chem. B* **2000**, *104*, 6942. (d) Cai, Z.; Gu, Z.; Sevilla, M. D. *J. Phys. Chem. B* **2000**, *104*, 10406.

(24) Dolgounitcheva, O.; Zakrzewski, V. G.; Ortiz, J. V. *J. Phys. Chem. A* **1999**, *103*, 7912.

(25) Foresman, J. B.; Frisch, M. J. *Exploring Chemistry with Electronic Structure Methods*, 2nd ed.; Gaussian, Inc.: Pittsburgh, PA, 1995–1996; p 143.

(26) (a) Close, D. M.; Sagtuen, E.; Hole, E. O.; Nelson, W. H. *J. Phys. Chem. B* **1999**, *103*, 3049. (b) Close, D. M. *Phys. Chem. Chem. Phys.* **2002**, *4*, 43.